

Lab-on-Chip for In Situ Analysis of Nutrients in the Deep Sea

Alexander D. Beaton,* Allison M. Schaap, Robin Pascal, Rudolf Hanz, Urska Martincic, Christopher L. Cardwell, Andrew Morris, Geraldine Clinton-Bailey, Kevin Saw, Susan E. Hartman, and Matthew C. Mowlem



Cite This: *ACS Sens.* 2022, 7, 89–98



Read Online

ACCESS |



Metrics & More

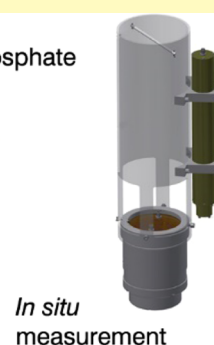
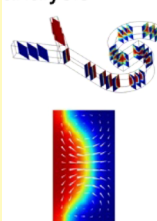


Article Recommendations

ABSTRACT: Microfluidic reagent-based nutrient sensors offer a promising technology to address the global undersampling of ocean chemistry but have so far not been shown to operate in the deep sea (>200 m). We report a new family of miniaturized lab-on-chip (LOC) colorimetric analyzers making in situ nitrate and phosphate measurements from the surface ocean to the deep sea (>4800 m). This new technology gives users a new low-cost, high-performance tool for measuring chemistry in hyperbaric environments. Using a combination of laboratory verification and field-based tests, we demonstrate that the analyzers are capable of in situ measurements during profiling that are comparable to laboratory-based analyses. The sensors feature a novel and efficient inertial-flow mixer that increases the mixing efficiency and reduces the back pressure and flushing time compared to a previously used serpentine mixing channel. Four separate replicate units of the nitrate and phosphate sensor were calibrated in the laboratory and showed an average limit of detection of $0.03 \mu\text{M}$ for nitrate and $0.016 \mu\text{M}$ for phosphate. Three on-chip optical absorption cell lengths provide a large linear range (to $>750 \mu\text{M}$ (10.5 mg/L-N) for nitrate and $>15 \mu\text{M}$ (0.47 mg/L-P) for phosphate), making the instruments suitable for typical concentrations in both ocean and freshwater aquatic environments. The LOC systems automatically collected a series of deep-sea nitrate and phosphate profiles in the northeast Atlantic while attached to a conductivity temperature depth (CTD) rosette, and the LOC nitrate sensor was attached to a PROVOR profiling float to conduct automated nitrate profiles in the Mediterranean Sea.

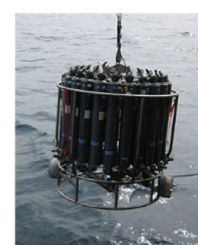
KEYWORDS: lab-on-chip, nutrients, sensors, nitrate, phosphate, in situ

Lab-on-chip
nitrate and phosphate
analysis



In situ
measurement

Deep sea
deployment



There have been major advances in the development of in situ oceanographic chemical sensors,¹ but it is still the case that the vast majority of ocean chemistry data are obtained using research ships to collect individual seawater samples that are either analyzed in shipboard laboratories or preserved and transported for later analysis on land. This approach is not only expensive and time consuming but results in low-resolution data sets, meaning that the world's ocean chemistry is heavily undersampled. High-resolution ocean chemistry data is essential for the development and validation of models and data products² that can help constrain biogeochemical cycles and predict future change, and for adding a biogeochemical element to ocean data assimilation systems.³

In situ chemical sensors and analyzers can provide high-quality, high-resolution data on a variety of biogeochemical parameters. Data from in situ sensors and analyzers can be made available immediately, rather than having to wait for analysis of samples in the laboratory, and can therefore be used to influence an environmental management response or research cruise tracks and deployment locations, without

requiring time and labor-intensive analysis. Integration of chemical sensors into observing stations, autonomous underwater vehicles (AUVs), and profiling floats allows the automated collection of chemical data (including depth profiles) over both spatial and temporal scales.⁴

For nitrate, UV-absorbance nitrate sensors (e.g., SUNA, Sea-Bird Scientific) have become commonplace, provide high-temporal-resolution data, and have been integrated into PROVOR, APEX, and Navis profiling floats.⁵ A network of biogeochemical sensor-enabled floats was deployed to estimate net community production in the Gulf of Alaska,⁶ while the larger SOCCUM array was used to estimate nitrate drawdown in the Southern Ocean.⁴ Over 30 000 nutrient profiles have

Received: August 8, 2021

Accepted: October 21, 2021

Published: January 12, 2022



been collected using UV-absorbance nitrate sensors on profiling floats.⁵ However, inaccuracies caused by drift (e.g., due to fouling) and offsets in initial calibrations (due to interferences from other variable chemistries in natural waters and instabilities during sensor transport and storage prior to deployment) mean data from float-mounted UV-absorbance nitrate sensors often have to be corrected using estimates of nitrate concentrations at or below 1500 m (where nitrate concentrations are considered relatively stable), obtained using interpolation methods⁷ from shipboard observations.⁴ As well as drift, these sensors have a depth rating (e.g., 2000 m SUNA Deep) based on the pressure housing, and the technology is limited in the number of parameters it can measure. While they have the advantages of high sampling rates and few or no moving parts, UV nitrate sensors generally fall short of wet chemical analyzers in terms of analytical performance, e.g., 0.3 μM limit of detection (LOD) for UV sensors (<https://www.seabird.com/nutrient-sensors/suna-v2-nitrate-sensor/>) vs 0.02 μM LOD for a wet chemical sensor⁸ and suffer from drift because large analytical volumes mean that they cannot easily perform in situ recalibration.

Sensitive colorimetric wet chemical assays are available for multiple parameters, and many of these (e.g., for nitrate, phosphate, and silicate) are used as the standard laboratory-based analysis methods for seawater.⁹ While demonstrating significantly better analytical performance than, for example, UV-absorbance nitrate sensors, and lending themselves naturally to in situ calibration, wet chemical analyzers suffer the drawbacks of generally being large/bulky, requiring liquid chemicals as consumables, and generating liquid chemical waste that either needs to be stored or expelled into the environment.

Several in situ wet chemical analyzers have been reported in the literature over the last 35 years,^{10–12} but recent work has shown that this technology can be miniaturized using microfluidics and lab-on-chip (LOC) techniques.^{13–15} Microfluidics involves the manipulation of fluid using channel dimensions on the submillimeter scale and presents major advantages in terms of size and resource (power and fluid) consumption. Lab-on-chip (LOC) refers to the miniaturization and automation of laboratory processes by combining microfluidics with small-scale sensors, actuators, and control systems. LOC approaches can be conveniently implemented via fluidic channels etched into a solid substrate (e.g., a polymer chip) and bonded to another layer to seal the channels.¹⁶ Low fluid consumption associated with microfluidics means that each measurement can be standardized if necessary, that blanks and standards can be performed as frequently or infrequently as desired (depending on the deployment scenario), and that liquid chemical waste is generated in such small volumes that it can sensibly be stored onboard the analyzer rather than being expelled into the environment. Deploying microfluidic sensors in the deep sea is not trivial^{17,18} due to low temperature and high hydrostatic pressure, but low size and resource consumption make microfluidic chemical analyzers candidates for integration into autonomous underwater vehicles and profiling floats, as well as long-term fixed platforms where power consumption and size are important limiting parameters.

Previous work has reported lab-on-chip nutrient analysis systems performing in situ measurements in a range of aquatic surface environments (estuaries,^{8,19} rivers²⁰ and glacial melt-water²¹) as well as shallow ocean deployments.^{22,23} Recently,

lab-on-chip nitrate analyzers have been deployed on Kongsberg Seagliders in shallow shelf seas.^{24,25} Here, we present the first demonstration of LOC platforms for in situ nitrate and phosphate analysis in the deep sea. We present the first deep (>200 m) in situ ocean nutrient profiles conducted using a LOC analyzer. The system described here is an improved version of that described by Beaton et al.⁸ and features several changes to improve the analytical performance (increase range and lower the LOD), increase the deployment endurance, and allow the sensor to operate at elevated hydrostatic pressures and low temperatures experienced in the deep sea. By integrating such a system with autonomous profiling platforms, inaccuracies in nitrate and other chemical profiles could be corrected, and the range of parameters measured by autonomous platforms can be expanded.

METHODS

Common Platform Hardware. Chip. The central component of the LOC platform is a round three-layer dark poly(methyl methacrylate) (PMMA) microfluidic chip (Figure 1A), which is

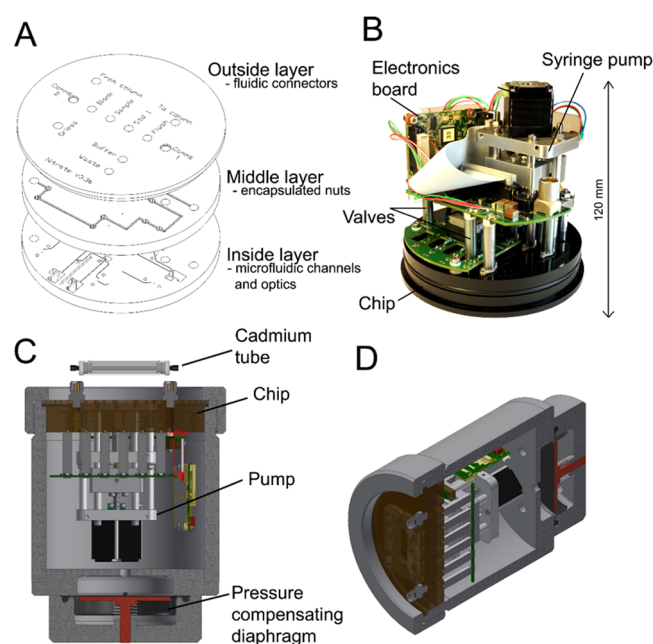


Figure 1. (A) Three layers of the microfluidic chip (119 mm diameter) shown prior to bonding. The outside layer contains tapped 1/4–28 fluidic ports, the middle layer contains encapsulated nuts for fixing the pump and valves, and the top layer contains the milled microfluidic channels, optical cells, light sources (LEDs), and detectors (photodiodes). (B) Photograph of the inside of the LOC sensor showing the chip, syringe pump, electronic board, and valves. (C, D) Cutaway computer-aided design (CAD) images of the oil-filled underwater sensor housing showing the location of the encapsulated cadmium reduction tube, the microfluidic chip, the syringe pump, and the pressure-compensating diaphragm.

created using computer-numerically controlled (CNC) micro-milling followed by a solvent bonding process.¹⁶ The chip also forms the endcap to the underwater housing (Figure 1C), which reduces flushing volume by minimizing the fluidic distance between ambient seawater and the internal fluidic channels of the chip. The inner and middle layers of the chip are made from tinted PMMA, which enhances the system's optical performance by absorbing stray light emitted by the light-emitting diodes (LEDs) that has not interacted with the sample.²⁶ The outer layer is made from opaque black PMMA to prevent external light from interfering with optical measurements.

Microfluidic channels (dimensions $160\ \mu\text{m} \times 300\ \mu\text{m}$) are milled into the top of the inner layer of the chip, which is bonded to the middle layer during the first bonding stage. After inspection for bonding defects, the outside layer is added during a second bonding stage. All fluidic connections (including the sample inlet) are made using 1/4–28 fluidic fittings (IDEX Super Flangeless) via tapped fluidic ports cut into the outside layer of the chip. Tubing (poly(tetrafluoroethylene) (PTFE), 1.6 mm OD \times 0.5 mm ID) connects the ports on the chip to the fluid storage bags (containing reagents and calibration standards), which are hung in a cylindrical plastic tube mounted above the sensor.

Fluidic Control. Fluid control is performed by nine normally closed solenoid valves (Lee Company LFN series) and a custom-made three-channel syringe pump, which all mount directly to the chip. A custom syringe pump was chosen in favor of peristaltic pumps to deliver reproducible flow rates irrespective of environmental conditions (e.g., temperature and ambient pressure), therefore helping to achieve consistent mixing between samples and reagents. Previous studies^{27–29} have shown flow rates from peristaltic pumps to vary with environmental conditions and contribute toward temperature effects. The syringe pump is actuated by a Haydon Kerk Size 11 stepper motor linear actuator, with magnetic field sensors (and a magnet mounted to the sliding plate) providing positional feedback. The valves and pump are fixed to the chip using screws and threaded rods connected to nuts that are encapsulated in recesses cut between the outside and middle layers of the chip. These recesses are linked by a channel and vented to the main housing to avoid encapsulated air pockets.

The sensor platform performs discrete colorimetric measurements using a stopped-flow fluidic architecture. The fluidic design of the nitrate variant is an improved and simplified version of that described by Beaton et al.⁸ and uses the Griess assay for colorimetric nitrate and nitrite determination. Briefly, each measurement fluid is passed through a reference cell for a background optical absorbance measurement before being mixed with a buffer solution (3.4 g/L imidazole, adjusted to pH 7.8 using hydrochloric acid) and entering an off-chip cadmium tube, which reduces nitrate to nitrite. The fluid then mixes with the color-forming Griess reagent in the measurement cells, where it resides for the color-forming reaction to occur, producing an intensely colored azo dye with an absorbance peak at 540 nm. The phosphate sensor variant was described by Clinton-Bailey et al.¹⁹. It uses a modified version of the colorimetric phosphomolybdenum blue (PMB) method, where orthophosphate and other labile phosphorous species react with molybdenum in an acidic medium to produce 12-molybdophosphoric acid, which is then reduced to phosphomolybdate blue. This solution has optical absorbance peaks at 700 and 880 nm.

Microfluidic Mixer. The microfluidic chip incorporates a passive microfluidic mixer that exploits secondary inertial flows^{30,31} to efficiently mix solutions on the chip in a compact, easily fabricated design. This replaces a previously used “serpentine” mixer¹³ that relied primarily on time-dependent diffusive mixing and has the advantages of reducing mixing time, fluidic back pressure, and flushing volume, thus reducing both the time required for each measurement and the energy required for pumping.

The design is based on that described by Al-Halhouli et al.³¹ with geometric modifications to suit the needs of this system. Specifically, the channel cross-section was modified to match the existing channels on the lab-on-chip system, and the dimensions of the pattern were modified to maximize mixing (e.g., the smallest possible radius of curvature) while remaining within the requirements imposed by the channel size, machining processes, and PMMA bonding process. Other Dean flow mixers have been used in various lab-on-chip devices, including split-channel designs or spirals.³² The strength of the approach used in our application is that it does not have split channels (which could prevent mixing if one channel arm gets a bubble in it), and the mostly linear design (compared to a larger spiral) allows for flexibility in the positioning of the mixer.

The mixer design relies on Dean flows: two counter-rotating secondary flows created when flow at a low but inertially relevant Reynolds numbers travels around a bend with a small radius of

curvature. The mixer design can be characterized by the Reynolds number

$$Re = \frac{\rho u x}{\mu}$$

where ρ is the fluid density, x is the characteristic channel hydraulic diameter, u is the speed of flow, and μ is the fluid viscosity, and the Dean number

$$De = Re \sqrt{\frac{x}{2R_{\text{curv}}}}$$

where R_{curv} is the radius of curvature of the bend. For $Re \sim 20$ – 200 and $De \sim 1$ – 100 , these secondary flows are reliably generated and perturb the interface between parallel laminar fluids, enhancing mixing.

Mixer design parameters were optimized using COMSOL simulations run over a range of flow rates (100–200 $\mu\text{L}/\text{min}$ per inlet), channel aspect ratios, radii of curvature, and fluid temperatures. Model results were quantified by calculating the standard deviation, σ , of the concentration of the fluid at all mesh points located at the outlet of the channel. To quantify the mixing results, the inlets were defined as having a concentration of a solution of either 0 or 1. The amount of mixing is defined by parameter $\alpha = 1 - 2\sigma$, where σ is the standard deviation of the concentration of the fluid at all mesh points at the channel outlet so that mixing along the channel progresses from $\alpha = 0$ ($\sigma = 0.5$, unmixed) to $\alpha = 1$ ($\sigma = 0$, fully mixed). Experimentally, mixing was quantified on a transparent PMMA microfluidic chip by mixing Tris buffer (colorless, pH 11.5) with phenolphthalein (colorless at low pH and red at pH > 10) and collecting monochromatic microscopy images illuminated with a green light. Experiments were performed at 20 °C (ambient room temperature) and 5 °C (in a cold-water bath) at flow rates 100–250 $\mu\text{L}/\text{min}$ per inlet (corresponding to $29 < Re < 72$ and $19 < De < 47$).

Operation at Depth. Operation at depth is enabled with an oil-filled hydraulically pressure-compensated housing (Figure 1C,D), and all internal components are selected or designed to survive and operate in mineral oil at 6000 m depth (i.e., pressure \sim 600 bar). This approach avoids the use of a bulky and expensive pressure resisting housing (e.g., gas filled at atmospheric pressure) to protect internal components. The sensor housing is filled with white mineral oil. A rolling diaphragm (Bellofram Corporation, West Virginia) fitted into the bottom of the housing compensates for the change in the volume of the oil as a function of ambient pressure and oil temperature. The diaphragm is permanently energized by a light compression spring that maintains a positive internal pressure of <0.05 bar to discourage water ingress. The spring is attached to a pin that extends outside the housing and is used to set the mid-position of the diaphragm when the housing is initially filled with oil (at room temperature and atmospheric pressure). The rolling diaphragm is able to compensate for both a 40 mL expansion of the oil at higher temperatures and a 60 mL contraction at lower temperatures and higher ambient pressures (a 60 mL volume decrease would occur between 20 °C and atmospheric pressure, and -20 °C and 600 bar). The oil-filled housing is sealed with an O-ring compressed against the housing by the PMMA chip, the latter forming the endcap. The nitrile rubber O-ring seal sits underneath a lip milled into the outside layer of the chip. This forms a face seal with the housing as it is compressed by rotating a cap onto a screw thread cut into the top of the housing.

Electronics and Software. The LOC sensors are operated by a custom pressure-tolerant electronics package consisting of three separate printed circuit boards (PCBs). The central processing board features an ARM SAM4L microcontroller, while two daughter boards perform pump/valve actuation and break out connections for LED control and analogue-to-digital channel inputs. Programming and downloading of raw data is conducted over USB via a Windows-based GUI, while a serial port (RS232 or RS485) transmits processed data in either streaming or polled mode (i.e., in response to an external request). A sleep mode allows the electronics package to enter a low-power mode between measurements, drawing <0.25 mA at 12 V.

When operating continuously, the average power consumption (dominated by the pump and valves) is 1.8 W.

Nitrate Sensor Variant. Typical operation of the LOC nitrate system consists of the measurement of a blank solution, followed by the sample solution (e.g., ambient seawater) and an onboard standard solution. Each measurement consists of a series of flushing steps performed by withdrawing and injecting the syringe pump, followed by a 50 s wait period for the chemical reaction to proceed. Each individual flush involves the injection of 60 μL of fluid per syringe channel. The first three flush cycles of each measurement are used for flushing the system with the new measurement fluid (blank, standard, or sample) and—in the case of the nitrate sensor—the buffer solution, while the color-forming reagents are unused and therefore returned to their storage bags from the pump, which has multiple simultaneously actuated syringes. On the fourth flush cycle, the color-forming reagents are injected into the chip along with the buffer (for nitrate) and measurement solution. When measuring a seawater sample (as opposed to a sample or blank), two additional flushing steps are performed prior to the measurement to flush the volume of fluid contained in the inlet filter (13 mm diameter 0.45 μm pore-size poly(ether sulfone) syringe filter). This mode of operation means that, per individual measurement, the nitrate sensor variant requires 240 μL of buffer solution, 60 μL of Griess reagent, and 360 μL of seawater sample.

Miniaturized Cadmium Tube. Nitrate is reduced to nitrite using a miniaturized copperized cadmium tube, which is manually activated prior to being fitted by flushing with hydrochloric acid and copper sulfate.⁹ This tube is connected to the outside of the chip housing via 1/4–28 connectors (chip side) and 062 MINSTAC connectors (tube side), which are bridged by two 20 mm long 0.3 mm internal diameter PTFE tubes. Locating the cadmium tube externally means that the sensor housing does not need to be opened if the cadmium tube needs to be changed or reconditioned. Seeing as the tube lies within the flushable fluidic path of the system (i.e., it has to be completely flushed with each new sample, blank or standard), it is critical to minimize the volume of both the cadmium tube and the connecting PTFE tubing. The miniaturized tube was created by compressing a 50 mm long cadmium tube so that it has an internal volume <80 μL . Flattening the tube maintains the water–Cd contact area while minimizing internal volume, and the length of the tube represents a compromise between flushable volume and reduction efficiency. The miniaturized cadmium tube has been shown to last for 1 year in both freshwater²⁰ and seawater before needing replacement.

Optical System. The nitrate chip contains three on-chip optical absorbance cells (92, 10, and 1 mm) arranged in series. LEDs (S25 nm; HLMP-CM1G-350DD, Avago Technologies, CA), and detection/monitoring photodiodes (TSLG257-LF, TAOS, TX) were aligned and fixed using optically clear epoxy (Opti-tec 5012, Intertronics, U.K.) into recesses milled into the chip in the same layer as the microfluidics, allowing light to be transmitted to and from the optical cell through 0.5 mm thick optical windows in the tinted PMMA.

LED output efficiency is affected by temperature. The LED temperature is affected by both ambient water temperatures (which could change rapidly during profiling), warming caused by heat dissipation from internal sensor components (e.g., stepper motor driving the pump and the solenoid-operated valves) and LED self-heating. While analysis of regular onboard standard solutions compensates for long-term (i.e., greater than one measurement cycle) drift in LED output, short-term drifts over the course of a measurement cycle (i.e., between the blank, sample, and standard) can translate into errors in measurements. LED optical output is therefore monitored using photodiodes mounted directly next to the emitting LED, allowing the signal received by the measuring photodiode to be corrected for changes in light source intensity.

Chemical Preparation. Reagents were prepared as per Beaton et al.⁹ (nitrate sensor) and Clinton-Bailey et al.¹⁹ (phosphate sensor), respectively, although for nitrate calibrations using nitrate concentrations higher than 100 μM , concentrations of sulfanilamide and *N*-(1-naphthyl)-ethylenediamine dihydrochloride were increased 5-fold

compared to those reported in Beaton et al.⁹ All glassware was soaked in 10% hydrochloric acid for at least 6 h and rinsed with Milli-Q (MQ) water before use. All standards and blanks were created using artificial seawater and serial dilution of stock solutions. A 5 mM nitrate stock solution was created by weighing out 0.5056 g of predried (105 °C for 1 h) analytical grade potassium nitrate and diluting it to 1000 mL with artificial seawater in a volumetric flask.

Calibration. Three identical LOC nitrate sensor units were calibrated at room temperature using standards of 0, 0.25, 2.5, 7.5, 10, 25, 50, 75, and 100 μM . One sensor was additionally calibrated using higher standards of 250, 500, and 750 μM . Three identical phosphate sensor units were calibrated using 0, 0.05, 0.1, 0.5, 1, 2.5, 5, 10, and 15 μM standards. For all sensors, the limit of detection and the limit of quantification were calculated as 3 times and 9 times the standard deviation of eight consecutive blank solutions, respectively.

Phosphate Sensor Variant. The phosphate optical detection system uses a 700 nm LED (LED700-02AU, Roithner) and optical cell lengths 92, 35, and 2.5 mm, but otherwise is the same as that of nitrate.

Reagents were prepared as per Clinton-Bailey et al.,¹⁹ using plasticware that was soaked in 10% hydrochloric acid for at least 6 h and rinsed with MQ water before use. One millimolar phosphate stock solution was created by weighing out 0.1361 g of predried analytical grade potassium dihydrogen phosphate and diluting it to 500 mL using artificial seawater and 3.2 mL of 5 M sulfuric acid. Phosphate standards were created by serial dilution from this stock.

The phosphate sensor was programmed to observe a waiting period of 300 s for the reaction to proceed once the new sample and reagents had been flushed into the measurement cells. For each individual measurement, the phosphate sensor required 60 μL of the ascorbic acid solution, 60 μL of molybdenum reagent, and 360 μL of seawater sample. The sensor was programmed to flush the optical cells with 0.01 M NaOH between measurements.

Three identical phosphate sensor units were calibrated using 0, 0.05, 0.1, 0.5, 1, 2.5, 5, 10, and 15 μM standards. Limit of detection and limit of quantification were calculated as 3 times and 9 times the standard deviation of eight consecutive blank solutions, respectively.

Deployment at Sea on Conductivity Temperature Depth (CTD) Rosette. The LOC nitrate and phosphate systems were attached to a conductivity temperature depth (CTD) rosette on the research vessel RRS James Cook on cruise JC165 to the Porcupine Abyssal Plain Sustained Observatory (PAP-SO), northeast Atlantic, in May–June 2018. The CTD rosette consists of a frame containing 24 Niskin sampling bottles that can be triggered at different depths, as well as instruments for measuring conductivity, temperature, and depth. Both systems were fitted with brackets that allowed them to be attached in place of 2 of the 24 Niskin sampling bottles (Figure 2B). For this

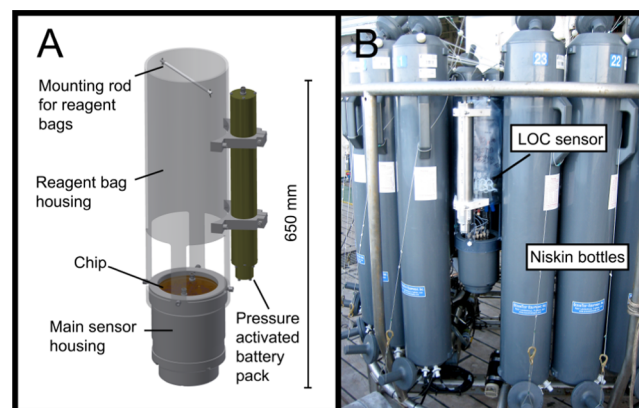


Figure 2. (A) CAD image of a fully assembled LOC sensor with pressure-activated battery pack, the reagent bag housing tube, and the mounting rod from which reagent bags were hung. (B) Photograph of the LOC sensor attached to the sampling rosette frame in place of 1 of the 24 Niskin sample bottles.

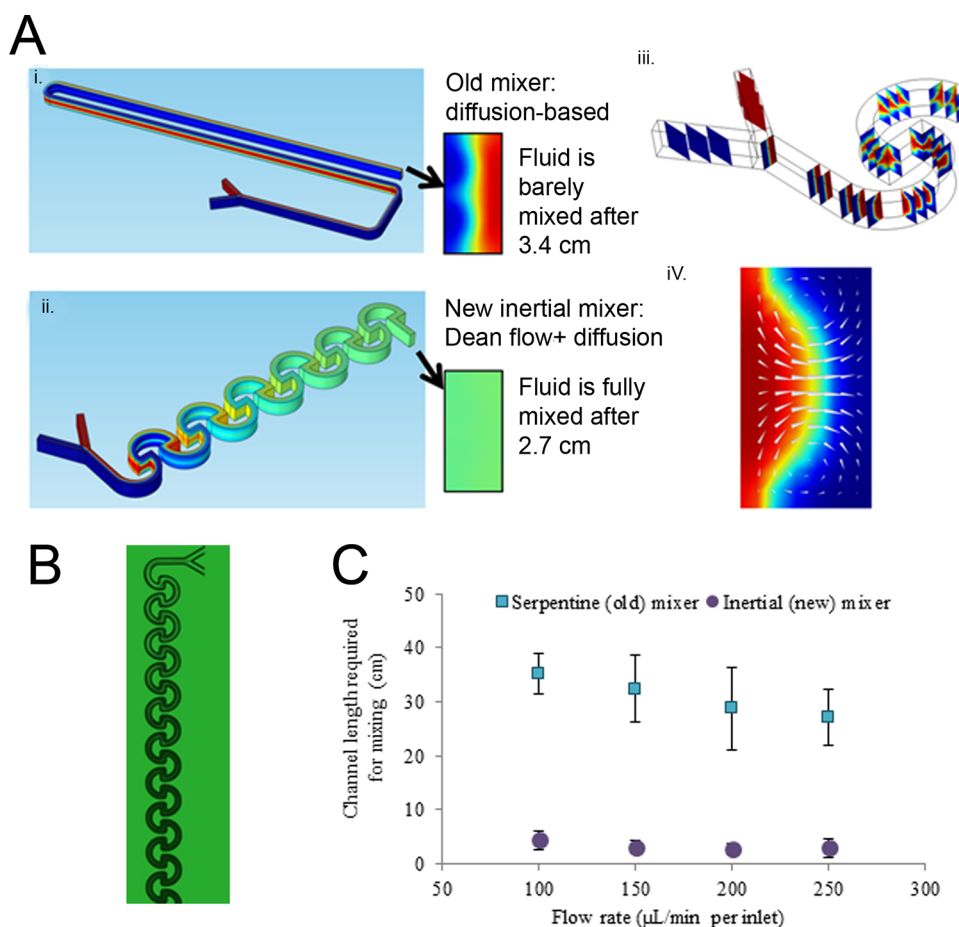


Figure 3. (A) Micromixer simulations: (i) a 3.4 cm long section of the original serpentine diffusion-based mixer and (ii) a 2.7 cm long section of the Dean flow-based micromixer. Both mixers have inlet flow rates of $150 \mu\text{L}/\text{min}$, a channel height of $300 \mu\text{m}$, a channel width of $160 \mu\text{m}$, and a concentration of zero (blue) in one inlet and one (red) in the other inlet. The diffusion coefficient of the red area is 5.5×10^{-10} which is an estimate of the diffusion coefficient of imidazole buffer at 2°C . (iii) Slices of concentrations show the effect of the counter-rotating Dean flows and (iv) shows the Dean flows (arrow lengths proportional to flow rate) in the cross-section of the channel at the apex of the first bend of the mixer. (B) Micrograph of the mixer during operation. The fluids being mixed are both transparent when entering the channel (top of image) and become opaque to green light when mixed (bottom of image). (C) Experimental results showing the channel length required for mixing (i.e., distance to maximum opacity) for the serpentine and inertial mixers over a range of flow rates.

deployment, each system was powered by four Saft LSH 20 3.6 V Li-SOCl₂ D cells connected in series. These were housed in titanium pressure housings (Figure 2A) rated to 6000 m and featuring pressure-activated switches set to engage the battery packs at a depth of 10 m. The LOC sensor was programmed to start measuring automatically when receiving power from the battery pack. This mode of operation meant that once set up and installed on the CTD rosette, the LOC systems required no user input for the duration of the cruise and could be left to automatically collect a profile for each deployment of the CTD (this battery pack allows each sensor to operate for 104 h continuously). On this cruise, two deep profiles (4800 m) were conducted with the sensors attached. The calibration and sampling sequence of the LOC sensors can be configured by the user. For this deployment, the nitrate sensor was programmed to conduct the following repeated sampling sequence: blank–sample–standard–sample, which resulted in a sample measurement every 11 min 20 s. The phosphate sensor was programmed to a measurement cycle consisting of a blank and two onboard standard solutions, followed by five consecutive seawater sample measurements, resulting in an interval of 5 min 50 s between each consecutive sample and a 21 min 39 s gap for each calibration procedure.

For comparison, water samples were collected from Niskin bottles that were closed at nine separate depths. These were immediately frozen and analyzed at a shore-based laboratory using a colorimetric segmented flow analyzer (QuAATro, Seal Analytical).

Deployment at Sea on PROVOR Float. The LOC nitrate system was attached via a custom-built frame to the outside of a PROVOR profiling float (see Figure 5D) and deployed in the Mediterranean Sea off Villefranche-sur-Mer on May 10, 2017. Additional prototype sensors developed as part of the SenseOCEAN project³³ were also attached to the float.³⁴

RESULTS

Inertial-Flow Mixer. The final optimized geometry of the new micromixer consisted of $160 \mu\text{m}$ wide and $300 \mu\text{m}$ deep channels in a series of circular patterns with a radius of curvature of 0.5 mm. In both simulations and experiments, the inertial-flow mixer showed significantly better mixing performance than the previously used serpentine mixer at all tested flow rates ($100\text{--}250 \mu\text{L}/\text{min}$) and temperatures (5 and 20°C , Figure 3).

In the COMSOL models of the original serpentine mixer, after 3.4 cm, the values of α were below 0.18 at 2°C for the lowest flow rate and decreased further at higher flow rates due to the lower diffusion time. In contrast, a 2.7 cm long inertial mixer at 2°C saw the mixing parameter α substantially improved, with $\alpha = 0.80$ at $100 \mu\text{L}/\text{min}$ per inlet and $\alpha = 0.85$ at $200 \mu\text{L}/\text{min}$ per inlet. This increase with flow rate was small

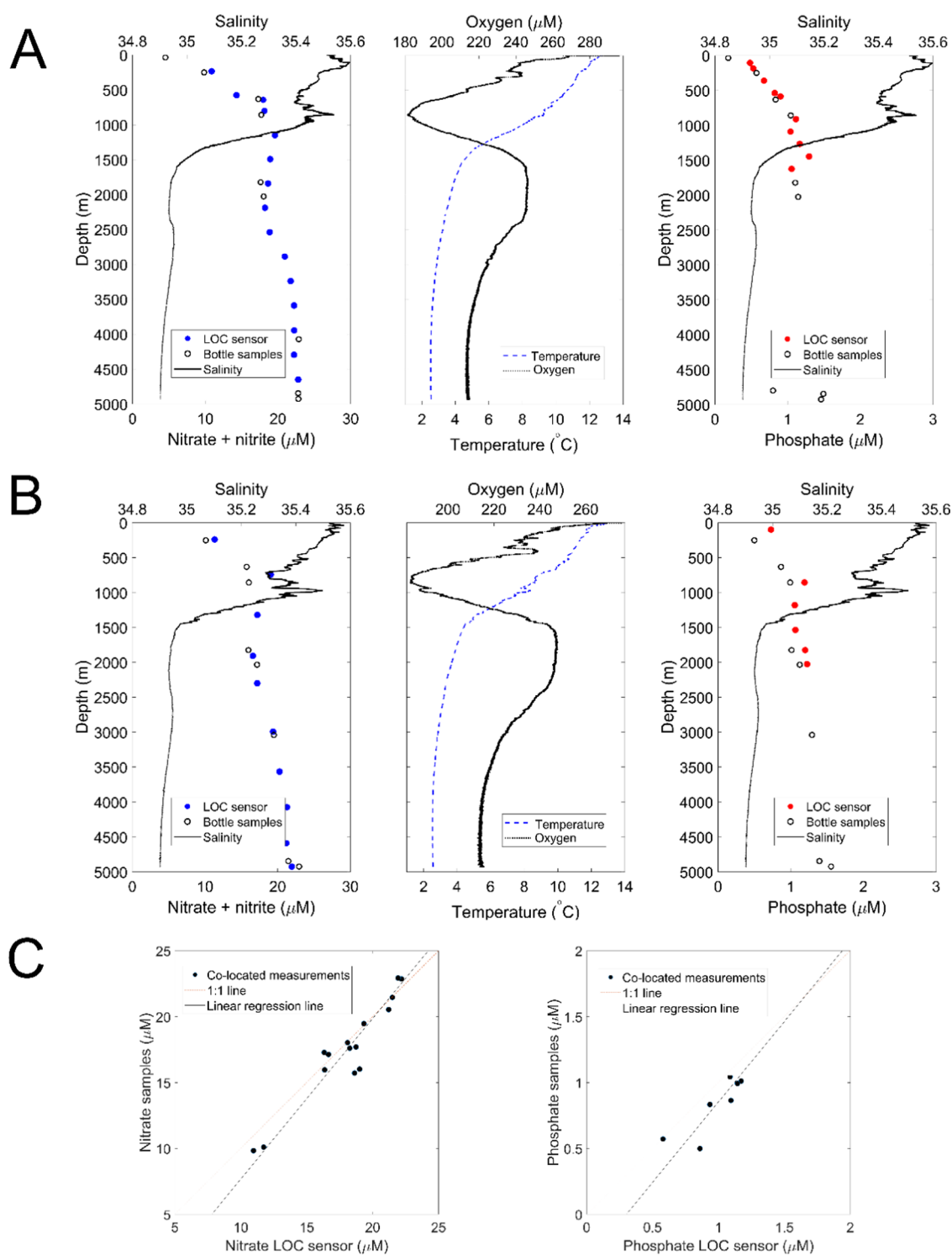


Figure 4. Data from deployment on CTD rosette for the first (A) and second (B) deep profiles. LOC sensor readings for nitrate (filled blue dots) and phosphate (filled red dots) are plotted on the same axes as the results from the bottle sample analysis (blank circles). Salinity, temperature, and dissolved oxygen data are also shown. (C) Linear regression between interpolated LOC sensor reading (x -axis) bottle sample analysis results (y -axis), showing the linear fit (dashed line) and 1:1 line (solid).

but significant: the higher flow rate results in a higher Dean number, indicating stronger secondary flows which increase the effectiveness of the mixer. Warmer temperatures also increase mixing efficiency: α reaches 0.9 at 200 $\mu\text{L}/\text{min}$ per inlet and 20 $^{\circ}\text{C}$. This results in a 2-fold effect, as higher temperatures increase the diffusion coefficient of the fluids as

well as decrease the fluid viscosity, which increases the Dean number and thus the magnitude of the secondary flows.

In the experiments with the inertial mixer design and fluid at 20 $^{\circ}\text{C}$, the distance required for mixing was 4.5 ± 1.7 cm at 100 $\mu\text{L}/\text{min}$ per inlet and 3.0 ± 1.7 cm at 250 $\mu\text{L}/\text{min}$ per inlet. These distances were 7.9 and 9.0 times shorter than those required for the serpentine mixer at the same flow rates (Figure

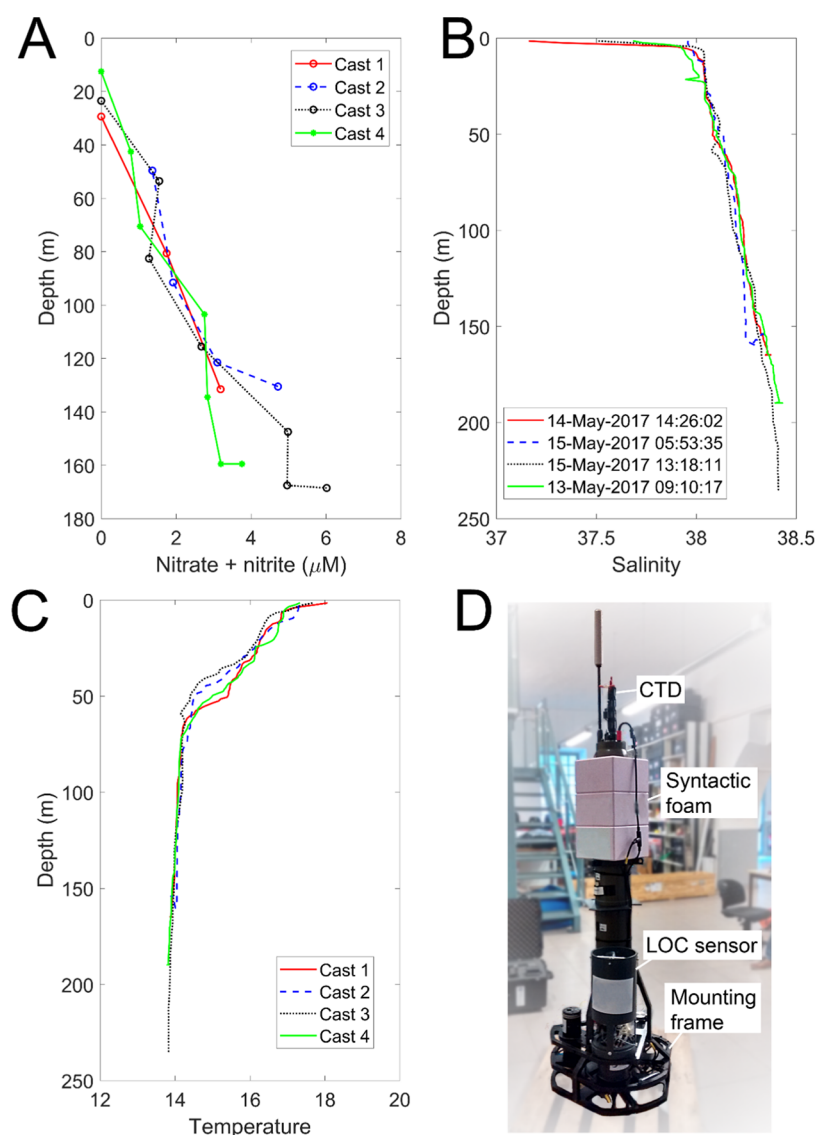


Figure 5. Data from deployment on PROVOR profiling float showing (A) nitrate + nitrite profiles from the LOC sensor. (B) Salinity profiles from the onboard CTD. (C) Temperature profiles from the onboard CTD. (D) Photograph of the PROVOR float prior to deployment showing the LOC sensor on its mounting frame, the syntactic foam used to ballast the vehicle, and the CTD.

3). At 5 °C, the distance required for mixing in the inertial mixer increases by a factor of 2. The final mixer used on the nitrate sensor consisted of 20 repeating patterns of the mixer geometry over a 9 cm channel length.

The new mixer is a significant improvement over the serpentine mixer. The reduction in overall channel length reduces the hydraulic resistance of the system, allowing for faster pumping speeds to be used. This decreases the time per measurement and also decreases the required energy per measurement by 22% as the pump uses a fixed current independent of pumping speed. The shorter channel length and decreased axial dispersion resulting from secondary flows allow a decrease in the amount of fluid used per measurement, saving on reagent consumption. Compared to other published work, it is a compact and easily fabricated design, which has been characterized over the range of oceanographically relevant temperatures (including lower temperatures at depth, as is the focus of this paper).

Limit of Detection and Range. The four nitrate sensors tested showed an average LOD of $0.030 \pm 0.005 \mu\text{M}$ (mean \pm

1σ) and LOQ of $0.091 \pm 0.0014 \mu\text{M}$ (mean $\pm 1\sigma$). All sensors showed an $R^2 > 0.99$ for the long channel up to $10 \mu\text{M}$, the medium channel up to $100 \mu\text{M}$, and (in the case of the one sensor tested over this range) the short channel up to $750 \mu\text{M}$. The four phosphate sensors showed an average LOD of $0.016 \mu\text{M}$ ($\sigma = 0.003 \mu\text{M}$) and LOQ of $0.062 \mu\text{M}$ ($\sigma = 0.033 \mu\text{M}$), with $R^2 > 0.99$ for the long channel up to $2.5 \mu\text{M}$ and the medium channel up to $15 \mu\text{M}$. While these tests show good consistency between multiple sensors of the same type in laboratory conditions, a combined uncertainty study by Birchill et al.³⁵ recently calculated a realistic combined measurement uncertainty of $<5\%$ for LOC nitrate sensors.

CTD Deployment. Sensor data for nitrate, phosphate, salinity, temperature, and oxygen were taken from the ascending profile of each cast (Figure 4A,B). Because Niskin bottle samples were not collected at exactly the same time as the LOC measurements, a high-order polynomial was fitted to the LOC data to generate interpolated colocated datapoints at the depths of the bottle samples. One clear bottle sample outlier (at 4800 m) was removed from the second profile.

Linear regression (Figure 4C) was used to compare the two methods (interpolated LOC and bottle sample) over the depth range that the LOC sensor sampled. The slope of the linear fit between LOC and bottle samples was not statistically different to 1 for both the nitrate (bottle sample = $(1.10 \pm 0.1) \times \text{LOC} - (2.38 \pm 1.8)$, $R^2 = 0.9$, $p < 0.05$, $n = 15$) and phosphate (bottle sample = $(0.86 \pm 0.24) \times \text{LOC} - (0.03 \pm 0.25)$, $R^2 = 0.72$, $p < 0.05$, $n = 7$) sensors.

The phosphate sensor stopped producing reliable data below 2160 m on deployment 1 and 2146 m on deployment 2, possibly due to a mechanical pump failure. Data below these depths were excluded from the analysis.

Despite this, these data demonstrate agreement of the LOC sensors to co-sampled reference measurements across a range of temperature, salinity, and dissolved oxygen concentrations.

Nitrate and phosphate were depleted in surface waters due to biological uptake, while variations in nitrate, salinity, temperature, and oxygen throughout the water column reflect the presence of several different water masses. Castrillejo et al.³⁶ present similar profiles of salinity, temperature, and oxygen from a nearby location, showing that warm and saline North Atlantic Central Water dominates the upper 500 m, with the salinity peak and oxygen minimum present at 1000 m due to the presence of northward-flowing Mediterranean Water. Below this peak, Labrador Sea Water is present, while slightly colder and saltier north-eastern Atlantic Deep Water exists below 2000 m.

PROVOR Float Deployment. The PROVOR float conducted five profiles with the LOC sensor turned on, descending to a maximum depth of 165.5 m with each profile containing up to seven measurements. One full nitrate profile was removed as an outlier, likely the result of a sensor malfunction. Nitrate concentrations ranged from 0 in the surface waters (between 12.5 and 29.4 m deep) to $6.02 \pm 0.30 \mu\text{M}$ at a depth of 165.5 m. The temperature ranged from 18.07 °C in the surface layer to 13.8 °C at 235 m depth, while salinity increased gradually with depth (to a maximum of 38.4) once the float had passed through a freshened surface layer.

While no colocated manual bottle samples could be collected during that deployment, nitrate concentrations recording by the LOC sensor are comparable to those reported by de Fommervault et al.³⁷ in their compilation of monthly nutrient data from the DYFAMED time-series station between 1991 and 2011. They report a decrease in nutrient concentrations in the surface layer in spring, with median nitrate concentrations of $0.28 \pm 0.33 \mu\text{M}$ in the 0–50 m depth interval and $8.14 \pm 0.52 \mu\text{M}$ in the 200–600 m depth interval in May (Figure 5).

DISCUSSION

This work describes miniaturized chemical analyzers that are capable of nutrient analysis in the deep sea (field proven to 4800 m (nitrate) and 2100 m (phosphate)). While wet chemical analyzers have previously been used for fixed platform deployments, here we demonstrate lab-on-chip sensors that are capable of oceanographic profiling applications, both ship tethered and via an autonomous platform. The sensors are rated to 6000 m and feature an oil-filled pressure-compensating housing that can compensate for changes in the volume of oil across the range of depths (0–6000 m) and temperatures (−2 to 40 °C) typically encountered in ocean scientific research. Although both deployments described here utilized research ships, the size and power requirements of the

LOC sensors make them suitable for integration with autonomous platforms such as Seagliders,²⁴ profiling floats (this study), and long-range AUVs (e.g., Autosub Long Range—ALR³⁸), many of which are capable of being launched from small vessels or, in the case of ALR, from the shore.

The miniaturization of wet chemical seawater analysis methods using microfluidics has the advantage of reducing both power and reagent consumption¹⁵ (thus widening the range of deployment scenarios) while still permitting the use of sensitive wet chemical colorimetric methods (which continue to be the mainstay of laboratory-based seawater nutrient analysis⁹). This allows the collection of high-quality data in a convenient and practical manner. The ability of these systems to carry onboard standards means that long-term drift can be compensated for as long as the concentration of the standard solution remains stable. A separate study (unpublished data) has shown nitrate standards (preserved with 0.1% chloroform) to be stable for over 1 year at 5 °C.

A 0.45 μm pore-size inlet filter prevents the introduction of any particles (e.g., algal clusters or marine snow) that may risk blocking the 150 μm wide microfluidic channels. The use of microfluidics means that a relatively low volume of sample (<1 mL) passes through the filter, allowing the systems to be operated for long periods (several thousand measurements in typical coastal waters) before requiring the filter to be changed.

While the deployments described here were relatively short in duration and therefore cannot be considered a test of resilience to biofouling, previous deployments in high-fouling coastal environments^{8,19} have demonstrated fouling of the microfluidic channels not to be an issue.

The key drawback of this approach is the length of time required for each measurement. In many deployment scenarios (e.g., on long-term fixed platform deployments where hourly or even daily sampling is considered sufficient), the shortest measurement interval currently provided by the LOC sensors (5–6 min) is adequate. However, for profiling applications on moving platforms, a shorter measurement interval would result in a more detailed nutrient profile and the potential for greater insight and understanding. No suitable technology has yet been demonstrated for higher temporal resolution ocean phosphate measurements. Advances in droplet microfluidics³⁹ have recently allowed the demonstration of very high-temporal-resolution in situ wet chemical nitrate analyzers, but short optical path lengths due to droplet size currently restrict these to high nutrient environments. UV-absorbance nitrate sensors (e.g., SUNA) can provide high-temporal-resolution nitrate measurements at the expense of poorer accuracy and long-term drift (due to inability to self-calibrate). The LOC wet chemical sensors described here could, for example, be used to perform lower temporal resolution but more frequently calibrated nitrate measurements to offer drift correction to high-temporal-resolution UV-absorbance measurements on profiling floats and other autonomous profiling platforms.

This work describes the first application of lab-on-chip sensor technology to nutrient analysis in the deep sea. While lab-on-chip nutrient analysis has previously been reported in the laboratory and shallow coastal deployments, field operation in extreme environments such as the deep sea represents a significant step forward in robustness. As in situ ocean nutrient sensor deployments become more widespread, common deployment standards⁴⁰ will be required to enhance data quality and aid its usability in global databases and models.

AUTHOR INFORMATION

Corresponding Author

Alexander D. Beaton – National Oceanography Centre, Southampton SO14 3ZH, United Kingdom; orcid.org/0000-0002-0206-7466; Email: a.beaton@noc.ac.uk

Authors

Allison M. Schaap – National Oceanography Centre, Southampton SO14 3ZH, United Kingdom
 Robin Pascal – National Oceanography Centre, Southampton SO14 3ZH, United Kingdom
 Rudolf Hanz – National Oceanography Centre, Southampton SO14 3ZH, United Kingdom
 Urska Martincic – National Oceanography Centre, Southampton SO14 3ZH, United Kingdom
 Christopher L. Cardwell – National Oceanography Centre, Southampton SO14 3ZH, United Kingdom
 Andrew Morris – National Oceanography Centre, Southampton SO14 3ZH, United Kingdom
 Geraldine Clinton-Bailey – National Oceanography Centre, Southampton SO14 3ZH, United Kingdom
 Kevin Saw – National Oceanography Centre, Southampton SO14 3ZH, United Kingdom
 Susan E. Hartman – National Oceanography Centre, Southampton SO14 3ZH, United Kingdom
 Matthew C. Mowlem – National Oceanography Centre, Southampton SO14 3ZH, United Kingdom

Complete contact information is available at:

<https://pubs.acs.org/10.1021/acssensors.1c01685>

Notes

The authors declare the following competing financial interest(s): ADB, RP, CC and MM are co-founders and employees of Clearwater Sensors. The remaining authors declare that the research was conducted in the absence of any commercial or financial relationships that could be construed as a potential conflict of interest.

ACKNOWLEDGMENTS

This work was supported by the European Union Seventh Framework Programme (FP7/2007-2013) under SenseOCEAN (grant agreement number 614141) and the UK Natural Environment Research Council capital program OCEANIDS via the AutoNuts project (NE/P020798/1). The JC165 cruise was supported by UKRI CLASS project (Climate Linked Atlantic Sector Science) NE/R015953/1 and Susan E. Hartman is supported by iFADO (EU Intereg project “Framework for the Atlantic Deep Ocean”) EAPA_165/2016. The authors give special thanks to the large number of colleagues who have supported the development of the lab-on-chip nutrient sensors over the years, in particular John Walk, Jake Ludgate, Jim Wyatt, David Owsianka, Gregory Slavik, Davi Uliana, Steven Shorter, and Robin Brown.

REFERENCES

- (1) Johnson, K. S.; Coletti, L. J. In Situ Ultraviolet Spectrophotometry for High Resolution and Long-Term Monitoring of Nitrate, Bromide and Bisulfide in the Ocean. *Deep Sea Res., Part I* **2002**, *49*, 1291–1305.
- (2) Olsen, A.; Key, R. M.; van Heuven, S.; Lauvset, S. K.; Velo, A.; Lin, X.; Schirnack, C.; Kozyr, A.; Tanhua, T.; Hoppema, M.; Jutterström, S.; et al. The Global Ocean Data Analysis Project version 2 (GLODAPv2) – an Internally Consistent Data Product for the World Ocean. *Earth Syst. Sci. Data* **2016**, *297*.
- (3) Brasseur, P.; Gruber, N.; Barciela, R.; Brander, K.; Doron, M.; El Moussaoui, A.; Hobday, A. J.; Huret, M.; Kremer, A.-S.; Lehodey, P.; Matear, R.; Moulin, C.; Murtugudde, R.; Senina, I.; Svendsen, E. Integrating Biogeochemistry and Ecology into Ocean Data Assimilation Systems. *Oceanography* **2009**, *22*, 206–215.
- (4) Johnson, K. S.; Plant, J. N.; Coletti, L. J.; Jannasch, H. W.; Sakamoto, C. M.; Riser, S. C.; Swift, D. D.; Williams, N. L.; Boss, E.; Haëntjens, N.; et al. Biogeochemical Sensor Performance in the SOCCOM Profiling Float Array. *J. Geophys. Res.: Oceans* **2017**, *122*, 6416–6436.
- (5) Bittig, H. C.; Maurer, T. L.; Plant, J. N.; Schmechtig, C.; Wong, A. P. S.; Claustre, H.; Trull, T. W.; Bhaskar, T. V. S. U.; Boss, E.; Dall’Olmo, G.; Organelli, E.; Poteau, A.; Johnson, K. S.; Hanstein, C.; Leymarie, E.; Le Reste, S.; Riser, S. C.; Rupan, A. R.; Taillandier, V.; Thierry, V.; Xing, X. A BGC-Argo Guide: Planning, Deployment, Data Handling and Usage Mission Considerations or the Global. *Front. Mar. Sci.* **2019**, *6*, No. 502.
- (6) Plant, J. N.; Johnson, K. S.; Sakamoto, C. M.; Jannasch, H. W.; Coletti, L. J.; Riser, S. C.; Swift, D. D. Net Community Production at Ocean Station Papa Observed with Nitrate and Oxygen Sensors on Profiling Floats. *Global Biogeochem. Cycles* **2016**, *30*, 859–879.
- (7) Carter, B. R.; Feely, R. A.; Williams, N. L.; Dickson, A. G.; Fong, M. B.; Takeshita, Y. Updated Methods for Global Locally Interpolated Estimation of Alkalinity, PH, and Nitrate. *Limnol. Oceanogr. Methods* **2018**, *16*, 119–131.
- (8) Beaton, A. D.; Cardwell, C. L.; Thomas, R. S.; Sieben, V. J.; Legiret, F. E.; Waugh, E. M.; Statham, P. J.; Mowlem, M. C.; Morgan, H. Lab-on-Chip Measurement of Nitrate and Nitrite for in Situ Analysis of Natural Waters. *Environ. Sci. Technol.* **2012**, *46*, 9548–9556.
- (9) Becker, S.; Aoyama, M.; Woodward, E. M. S.; Bakker, K.; Coverly, S.; Mahaffey, C.; Tanhua, T. GO-SHIP Repeat Hydrography Nutrient Manual: The Precise and Accurate Determination of Dissolved Inorganic Nutrients in Seawater, Using Continuous Flow Analysis Methods. *Front. Mar. Sci.* **2019**, No. 581790.
- (10) Johnson, K. S.; Beehler, C. L.; Sakamoto-Arnold, C. M. A Submersible Flow Analysis System. *Anal. Chim. Acta* **1986**, *179*, 245–257.
- (11) Thouron, D.; Vuillemin, R.; Philippon, X.; Lourenço, A.; Provost, C.; Cruzado, A.; Garçon, V. An Autonomous Nutrient Analyzer for Oceanic Long-Term in Situ Biogeochemical Monitoring. *Anal. Chem.* **2003**, *75*, 2601–2609.
- (12) Jannasch, H.; Johnson, K.; Sakamoto, C. Submersible, Osmotically Pumped Analyzer for Continuous Determination of Nitrate in Situ. *Anal. Chem.* **1994**, *66*, 3352–3361.
- (13) Sieben, V. J.; Floquet, C. F. A.; Ogilvie, I. R. G.; Mowlem, M. C.; Morgan, H. Microfluidic Colourimetric Chemical Analysis System: Application to Nitrite Detection. *Anal. Methods* **2010**, *2*, 484–491.
- (14) Beaton, A. D.; Sieben, V. J.; Floquet, C. F. A.; Waugh, E. M.; Bey, S. A. K.; Ogilvie, I. R. G.; Mowlem, M. C.; Morgan, H. An Automated Microfluidic Colourimetric Sensor Applied in Situ to Determine Nitrite Concentration. *Sens. Actuators, B* **2011**, *156*, 1009–1014.
- (15) Nightingale, A. M.; Beaton, A. D.; Mowlem, M. C. Trends in Microfluidic Systems for in Situ Chemical Analysis of Natural Waters. *Sens. Actuators, B* **2015**, *221*, 1398–1405.
- (16) Ogilvie, I. R. G.; Sieben, V. J.; Floquet, C. F. A.; Zmijan, R.; Mowlem, M. C.; Morgan, H. Reduction of Surface Roughness for Optical Quality Microfluidic Devices in PMMA and COC. *J. Micromech. Microeng.* **2010**, *20*, No. 065016.
- (17) Fukuba, T.; Noguchi, T.; Okamura, K.; Fujii, T. Adenosine Triphosphate Measurement in Deep Sea Using a Microfluidic Device. *Micromachines* **2018**, *9*, No. 370.
- (18) Provin, C.; Fukuba, T.; Okamura, K.; Fujii, T. An Integrated Microfluidic System for Manganese Anomaly Detection Based on Chemiluminescence: Description and Practical Use to Discover

Hydrothermal Plumes near the Okinawa Trough. *IEEE J. Oceanic Eng.* **2013**, *38*, 178–185.

(19) Clinton-Bailey, G. S.; Grand, M. M.; Beaton, A. D.; Nightingale, A. M.; Owsianka, D. R.; Slavik, G. J.; Connelly, D. P.; Cardwell, C. L.; Mowlem, M. C. A Lab-on-Chip Analyzer for in Situ Measurement of Soluble Reactive Phosphate: Improved Phosphate Blue Assay and Application to Fluvial Monitoring. *Environ. Sci. Technol.* **2017**, *51*, 9989–9995.

(20) Beaton, A. D.; Mowlem, M. C.; Purdie, D. A.; Panton, A.; Owsianka, D. R. *Nitrate and Nitrite Data from a National Oceanography Centre (NOC) Lab-on-Chip (LOC) Analyser at Knapp Mill (Hampshire Avon)*; British Oceanographic Data Centre, Natural Environment Research Council: U.K., 2017.

(21) Beaton, A. D.; Wadham, J. L.; Hawkings, J.; Bagshaw, E. A.; Lamarche-Gagnon, G.; Mowlem, M. C.; Tranter, M. High-Resolution in Situ Measurement of Nitrate in Runoff from the Greenland Ice Sheet. *Environ. Sci. Technol.* **2017**, *51*, 12518–12527.

(22) Yücel, M.; Beaton, A. D.; Dengler, M.; Mowlem, M. C.; Sohl, F.; Sommer, S. Nitrate and Nitrite Variability at the Seafloor of an Oxygen Minimum Zone Revealed by a Novel Microfluidic In-Situ Chemical Sensor. *PLoS One* **2015**, *10*, No. e0132785.

(23) Milani, A.; Stathamb, P. J.; Mowlem, M. C.; Connelly, D. P. An In-Situ Microfluidic System for the Determination of FeII and Mn in Natural Waters. *Talanta* **2015**, *15*.

(24) Vincent, A. G.; Pascal, R. W.; Beaton, A. D.; Walk, J.; Hopkins, J. E.; Woodward, E. M. S.; Mowlem, M.; Lohan, M. C. Nitrate Drawdown during a Shelf Sea Spring Bloom Revealed Using a Novel Microfluidic in Situ Chemical Sensor Deployed within an Autonomous Underwater Glider. *Mar. Chem.* **2018**, *205*, 29–36.

(25) Birchill, A. J.; Beaton, A. D.; Hull, T.; Kaiser, J.; Mowlem, M.; Pascal, R.; Schaap, A.; Voynova, Y. G.; Williams, C.; Palmer, M. Exploring Ocean Biogeochemistry Using a Lab-on-Chip Phosphate Analyser on an Underwater Glider. *Front. Mar. Sci.* **2021**, *8*, No. 698102.

(26) Floquet, C. F. A.; Sieben, V. J.; Milani, A.; Joly, E. P.; Ogilvie, I. R. G.; Morgan, H.; Mowlem, M. C. Nanomolar Detection with High Sensitivity Microfluidic Absorption Cells Manufactured in Tinted PMMA for Chemical Analysis. *Talanta* **2011**, *84*, 235–239.

(27) Laës, A.; Vuillemin, R.; Leilde, B.; Sarthou, G.; Bournot-Marec, C.; Blain, S. Impact of Environmental Factors on in Situ Determination of Iron in Seawater by Flow Injection Analysis. *Mar. Chem.* **2005**, *97*, 347–356.

(28) Daniel, A.; Birot, D.; Blain, S.; Tréguer, P.; Leïldé, B.; Menut, E. A Submersible Flow-Injection Analyser for the in-Situ Determination of Nitrite and Nitrate in Coastal Waters. *Mar. Chem.* **1995**, *51*, 67–77.

(29) Daniel, A.; Birot, D.; Lehaitre, M.; Poncin, J. Characterization and Reduction of Interferences in Flow-Injection Analysis for the in Situ Determination of Nitrate and Nitrite in Sea Water. *Anal. Chim. Acta* **1995**, *308*, 413–424.

(30) Howell, P. B., Jr.; Mott, D. R.; Golden, P.; Ligler, F. S. Design and Evaluation of a Dean Vortex-Based Micromixer. *Lab Chip* **2004**, *4*, 663–669.

(31) Al-Halhouli, A.; Alshare, A.; Mohsen, M.; Matar, M.; Dietzel, A.; Büttgenbach, S. Passive Micromixers with Interlocking Semi-Circle and Omega-Shaped Modules: Experiments and Simulations. *Micromachines* **2015**, *6*, 953–968.

(32) Lee, C. Y.; Wang, W. T.; Liu, C. C.; Fu, L. M. Passive Mixers in Microfluidic Systems: A Review. *Chem. Eng. J.* **2016**, *288*, 146–160.

(33) Barus, C. *Policy Document—Sensor Development for the Ocean of Tomorrow*, [SenseOCEAN: Marine Sensors for the 21st Century, Deliverable 7.8]; National Oceanography Centre for SenseOCEAN: Southampton, U.K., 2017.

(34) Barus, C.; Legrand, D. C.; Striebig, N.; Jugeau, B.; David, A.; Valladares, M.; Parra, P. M.; Ramos, M. E.; et al. First Deployment and Validation of in Situ Silicate Electrochemical Sensor in Seawater. *Front. Mar. Sci.* **2018**, *5*, No. 60.

(35) Birchill, A. J.; Clinton-Bailey, G.; Hanz, R.; Mawji, E.; Cariou, T.; White, C.; Ussher, S. J.; Worsfold, P. J.; Achterberg, E. P.;

Mowlem, M. Realistic Measurement Uncertainties for Marine Macronutrient Measurements Conducted Using Gas Segmented Flow and Lab-on-Chip Techniques. *Talanta* **2019**, *200*, 228–235.

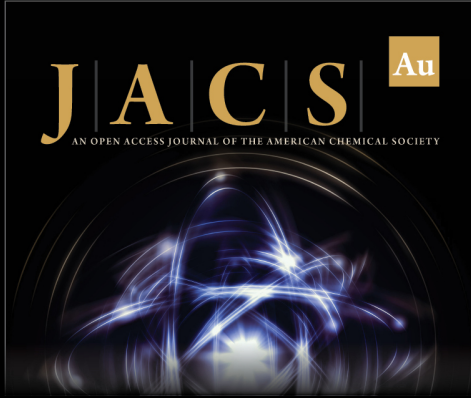
(36) Castrillejo, M.; Casacuberta, N.; Christl, M.; Vockenhuber, C.; Synall, H. A.; García-Ibáñez, M. I.; Lherminier, P.; Sarthou, G.; Garcia-Orellana, J.; Masqué, P. Tracing Water Masses with 129I and 236U in the Subpolar North Atlantic along the GEOTRACES GA01 Section. *Biogeosciences* **2018**, *15*, 5545–5564.

(37) de Fommervault, O. P.; Migon, C.; D'Ortenzio, F.; Ribera d'Alcalà, M.; Coppola, L. Temporal Variability of Nutrient Concentrations in the Northwestern Mediterranean Sea (DYFAMED Time-Series Station). *Deep Sea Res., Part I* **2015**, *100*, 1–12.

(38) Furlong, M. E.; Paxton, D.; Stevenson, P.; Pebody, M.; Mcphail, S. D.; Perrett, J. In *Autosub Long Range: A Long Range Deep Diving AUV for Ocean Monitoring*, 2012 IEEE/OES Autonomous Underwater Vehicles (AUV); IEEE, 2012.


(39) Nightingale, A. M.; Hassan, S.; Warren, B. M.; Makris, K.; Evans, G. W. H.; Papadopoulou, E.; Coleman, S.; Niu, X. A Droplet Micro Fluidic-Based Sensor for Simultaneous in Situ Monitoring of Nitrate and Nitrite in Natural Waters. *Environ. Sci. Technol.* **2019**, *9677*.


(40) Daniel, A.; Laës-Huon, A.; Barus, C.; Beaton, A. D.; Blandford, D.; Guigues, N.; Knockaert, M.; Muraron, D.; Salter, I.; Woodward, E. M. S.; et al. Toward a Harmonization for Using in Situ Nutrient Sensors in the Marine Environment. *Front. Mar. Sci.* **2020**, *6*, No. 773.



JACS Au
AN OPEN ACCESS JOURNAL OF THE AMERICAN CHEMICAL SOCIETY

Editor-in-Chief
Prof. Christopher W. Jones
Georgia Institute of Technology, USA

Open for Submissions 

pubs.acs.org/jacsau  ACS Publications
Most Trusted. Most Cited. Most Read.